

## Supporting information

for

### ***In-Situ* Synthesis of Titanium Doped Hybrid Metal-Organic framework UiO-66 with Enhanced Adsorption Capacity for Organic Dye**

Yitong Han<sup>a</sup>, Min Liu<sup>a</sup>, Keyan Li<sup>a</sup>, Qiao Sun<sup>a</sup>, Wensheng Zhang<sup>a</sup>, Chunshan Song<sup>ab</sup>, Guoliang Zhang<sup>c</sup>, Z. Conrad Zhang<sup>d\*</sup> and Xinwen Guo<sup>a\*</sup>

<sup>a</sup> State Key Laboratory of Fine Chemicals, PSU-DUT Joint Center for Energy Research, School of Chemical Engineering, Dalian University of Technology, Dalian 116024, PR China

<sup>b</sup> EMS Energy Institute, PSU-DUT Joint Center for Energy Research and Department of Energy & Mineral Engineering, Pennsylvania State University, University Park, Pennsylvania 16802, United States

<sup>c</sup> College of Biological and Environmental Engineering, Zhejiang University of Technology, Hangzhou 310014, PR China

<sup>d</sup> Dalian National Laboratory for Clean Energy, Dalian Institute of Chemical Physics, Chinese Academy of Sciences, Dalian 116023, PR China

\* Corresponding authors, (X.G.) E-mail: guoxw@dlut.edu.cn, Fax: +86-0411-84986134, Tel: +86-0411-84986133; (Z.Z.) E-mail: zczhang@yahoo.com, Fax: +86-0411-84379462, Tel: +86-0411-84379462.

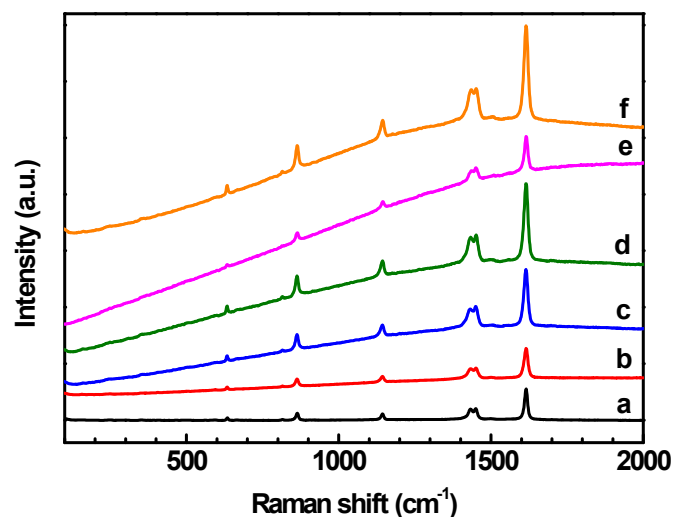


Fig. S1 Raman spectra of the parent UiO-66 (a), UiO-66-0.7Ti (b), UiO-66-1.4Ti (c), UiO-66-2.1Ti (d), UiO-66-2.7Ti (e) and UiO-66-4.0Ti (f), the excitation wavelength is 532 nm.

The Raman spectrum of an anatase-phase  $\text{TiO}_2$  is a combination of six peaks appear at  $144 \text{ cm}^{-1}$ ,  $197 \text{ cm}^{-1}$ ,  $399 \text{ cm}^{-1}$ ,  $513 \text{ cm}^{-1}$ ,  $519 \text{ cm}^{-1}$  and  $640 \text{ cm}^{-1}$ .<sup>1</sup> Therefore, as illustrated in Fig. S1, the Raman spectrum of the  $\text{Ti}^{4+}$  doped UiO-66 samples only show the common features seen for the parent UiO-66,<sup>2</sup> demonstrating the pure phase of the samples.

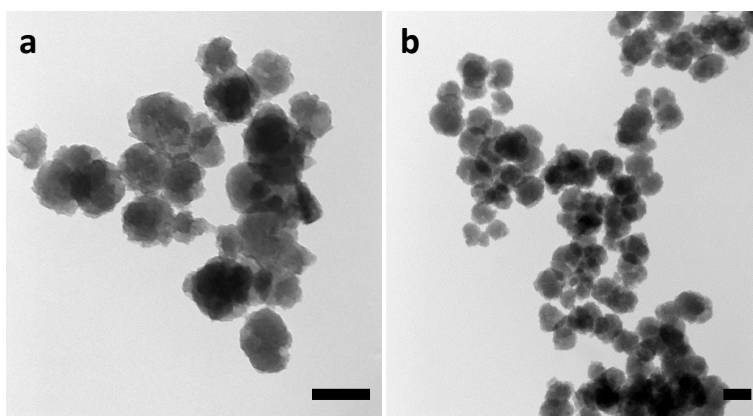


Fig. S2 TEM images of UiO-66-2.7Ti with different magnification. (a)  $20 \times 10^4$ , (b)  $10 \times 10^4$ , each scale bar is 100 nm.

Table S1 XPS data for the surface Ti/Zr molar ratio in the UiO-66-nTi MOFs.

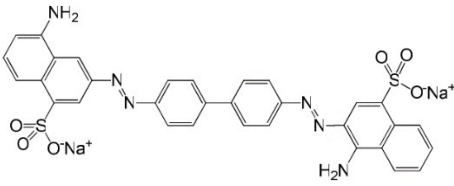
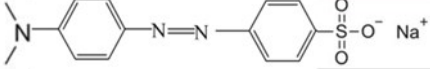
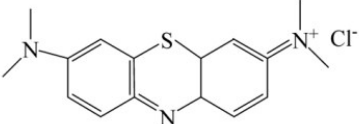
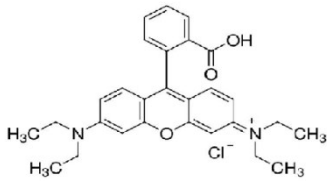
Sample	XPS for the surface
	Ti/Zr molar ratio (%)
UiO-66-0.7Ti	8.6
UiO-66-1.4Ti	17.2
UiO-66-2.1Ti	15.7
UiO-66-2.7Ti	16.1
UiO-66-4.0Ti	17.3

Table S2 Comparison of weight loss values (%) of the synthesized samples at different temperature interval.

Sample	Weight loss temperature interval (°C)			Stoichiometric <sup>a</sup> 450–700 °C
	Measured (%)			
	30–200	200–350	450–700	
UiO-66	1.9	10.6	43.5	54.6 <sup>3</sup>
UiO-66-0.7Ti	3.9	7.3	42.2	-
UiO-66-1.4Ti	5.0	7.1	38.2	-
UiO-66-2.1Ti	6.0	7.2	39.3	-
UiO-66-2.7Ti	6.3	7.3	35.9	-
UiO-66-4.0Ti	1.3	7.5	37.7	-

<sup>a</sup> stoichiometrically perfect framework

Table S3 Dyes used in the adsorption experiments in this work. <sup>4-6</sup>

	Structure	Molecular Formula	Mw
Congo Red	 $(20.2 \times 10.1 \times 10.2 \text{ \AA})$	$C_{32}H_{22}N_6Na_2O_6S_2$	697
Methyl Orange	 $(13.1 \times 5.5 \times 1.8 \text{ \AA})$	$C_{14}H_{14}N_3SO_3Na$	327
Methylene Blue	 $(13.9 \times 5.0 \times 4.3 \text{ \AA})$	$C_{16}H_{18}N_3SCl$	320
Rhodamine B	 $(15.9 \times 11.8 \times 5.6 \text{ \AA})$	$C_{28}H_{31}N_2O_3Cl$	479

### Adsorption Kinetics

The experimental data of the adsorption of CR ( $400 \text{ mg}\cdot\text{L}^{-1}$ ) on the parent UiO-66 and UiO-66-2.7Ti were fit by pseudo-first-order and pseudo-second-order kinetic equations to investigate the adsorption kinetic.

Pseudo-first-order equation:  $\ln(Q_e - Q_t) = \ln Q_e - k_1 t$  (1)

Pseudo-second-order equation:  $\frac{t}{Q_t} = \frac{1}{k_2} \cdot \frac{1}{Q_e^2} + \frac{t}{Q_e}$  (2)

where  $Q_e$  ( $\text{mg}\cdot\text{g}^{-1}$ ) is the equilibrium adsorption capacity,  $Q_t$  ( $\text{mg}\cdot\text{g}^{-1}$ ) is the adsorption capacity at time  $t$  (min), and  $k_1$  ( $\text{min}^{-1}$ ) and  $k_2$  ( $\text{g}\cdot\text{min}^{-1}\cdot\text{mg}^{-1}$ ) are rate constants of the pseudo-first-order and pseudo-second-order equations, respectively.

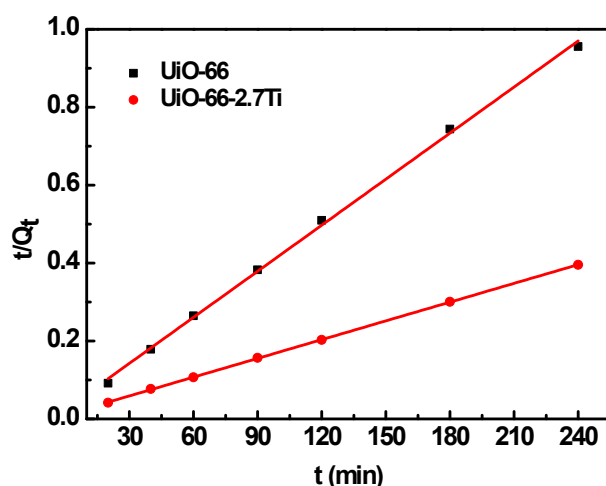


Fig. S3 Plots of pseudo-second-order kinetics for the adsorption of CR on the parent UiO-66 and UiO-66-2.7Ti.

Table S4 Kinetic parameters of the adsorption of CR on the parent UiO-66 and UiO-66-2.7Ti.

Sample	$Q_{e, \text{exp}}$ ( $\text{mg} \cdot \text{g}^{-1}$ )	Pseudo-first-order-model			Pseudo-second-order-model		
		$Q_{e, \text{cal}}$ ( $\text{mg} \cdot \text{g}^{-1}$ )	$k_1$ ( $\text{min}^{-1}$ )	$R^2$	$Q_{e, \text{cal}}$ ( $\text{mg} \cdot \text{g}^{-1}$ )	$k_2$ ( $\text{g} \cdot \text{min}^{-1}$ $\cdot \text{mg}^{-1}$ )	$R^2$
UiO-66	251	68	0.0163	0.4993	256	$6.2536 \times 10^{-4}$	0.9987
UiO-66-2.7Ti	607	557	0.0412	0.7112	625	$2.3681 \times 10^{-4}$	0.9999

### Adsorption Isotherms

Langmuir and Freundlich equations were used for describing the adsorption of CR on the samples.

$$\frac{C_e}{Q_e} = \frac{1}{K_l} \cdot \frac{1}{Q_m} + \frac{C_e}{Q_m}$$

The Langmuir equation: (3)

$$\ln Q_e = \ln K_f + \frac{1}{n} \cdot \ln C_e$$

The Freundlich equation: (4)

where  $C_e$  ( $\text{mg} \cdot \text{L}^{-1}$ ) is equilibrium concentration of dye solution,  $Q_e$  ( $\text{mg} \cdot \text{g}^{-1}$ ) is the amount adsorbed at equilibrium,  $Q_m$  ( $\text{mg} \cdot \text{g}^{-1}$ ) represents the adsorption capacity limit

of CR per unit mass of adsorbent,  $K_l$  ( $L \cdot mg^{-1}$ ) is a Langmuir constant which indicates the affinity of CR toward the adsorbent.  $K_f$  ( $mg^{1-1/n} \cdot L^{1/n} \cdot g^{-1}$ ) and  $1/n$  are Freundlich constants, related to adsorption capacity and adsorption intensity, respectively.

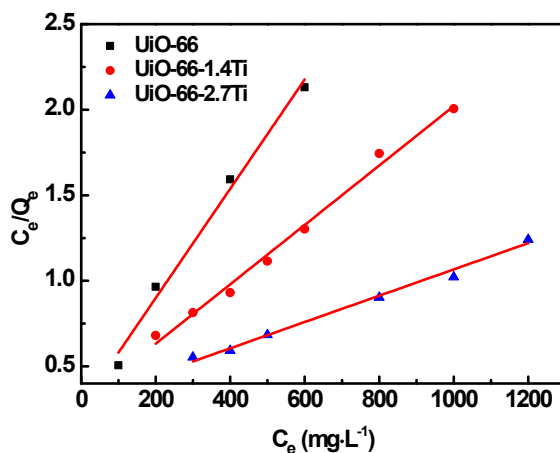


Fig. S4 Langmuir plots of isotherms for the adsorption of CR on the parent UiO-66, UiO-66-1.4Ti and UiO-66-2.7Ti.

Table S5 Langmuir and Freundlich model parameters of the adsorption of CR on the parent UiO-66, UiO-66-1.4Ti and UiO-66-2.7Ti.

sample	Langmuir isotherm			Freundlich isotherm		
	$Q_m$ ( $mg \cdot g^{-1}$ )	$K_l$ ( $L \cdot mg^{-1}$ )	$R^2$	$K_f$ ( $mg^{1-1/n} L^{1/n} g^{-1}$ )	$n$	$R^2$
UiO-66	313	0.0122	0.9853	88.4626	5.6863	0.1249
UiO-66-1.4Ti	575	0.0061	0.9901	58.9241	3.1326	0.8382
UiO-66-2.7Ti	1315	0.0025	0.9892	29.8144	1.9903	0.9537

#### *Synthesis of sample UiO-66(Ti)*

UiO-66(Ti) was synthesized via a modified post-grafting method. TOPT was mixed with 0.2 g the as-synthesized parent UiO-66 in 20 mL of toluene, and then the mixture was heated at 110 °C for 24 h. In order to compare the adsorption capacity with UiO-66-2.7Ti, the feeding molar ratio of Ti/Zr in the synthesis was 20% (the

mass percentage of Zr in the parent UiO-66 was calculated by the TGA data). After the treatment, the obtained sample was washed by toluene and methanol for several times and dried at 60 °C under vacuum.

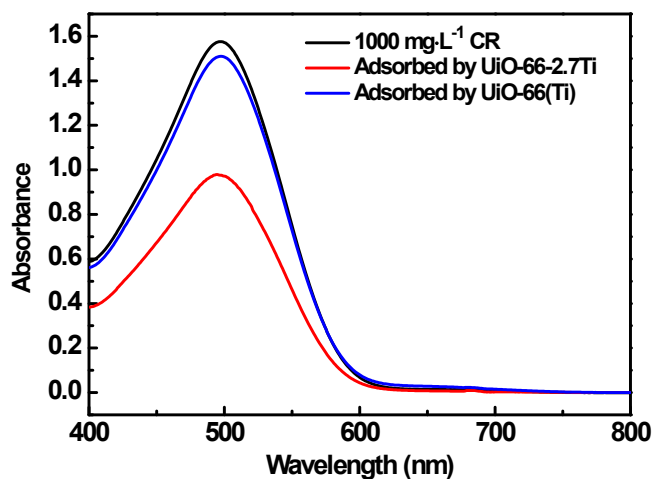


Fig. S5 UV-vis adsorption spectra of CR before (black curve) and after (red and blue curves) adsorption treatment with UiO-66-2.7Ti and UiO-66(Ti) ( $t = 4$  h,  $\text{pH} = 7$ ,  $\text{dyes} = 1000 \text{ mg}\cdot\text{L}^{-1}$ ,  $\text{does} = 0.5 \text{ g}\cdot\text{L}^{-1}$ ,  $T = 35 \text{ }^\circ\text{C}$ ).

Table S6 Zeta potentials of the synthesized samples in ultrapure water ( $\text{pH} = 7$ ).

Sample	Zeta potentials (mV)
UiO-66	-10.2
UiO-66-0.7Ti	4.8
UiO-66-1.4Ti	25.9
UiO-66-2.1Ti	57.1
UiO-66-2.7Ti	59.2
UiO-66-4.0Ti	60.0

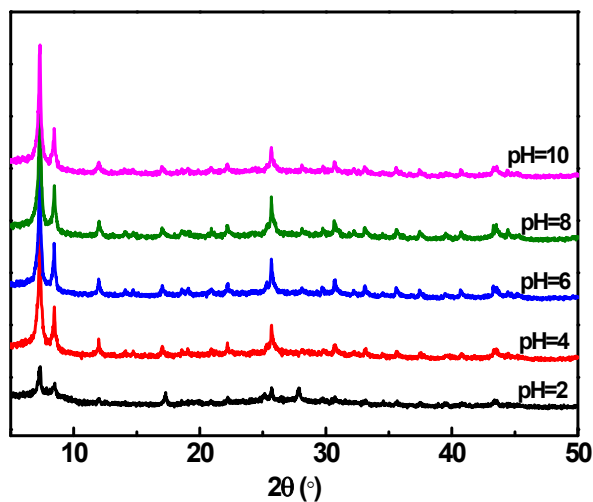


Fig. S6 XRD patterns of UiO-66-2.7Ti after the adsorption of CR at various pHs.

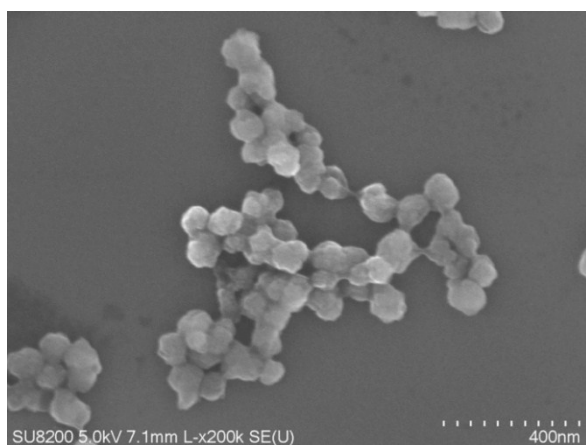


Fig. S7 SEM image of CR-adsorbed UiO-66-2.7Ti.

## References

- 1 H. C. Choi, Y. M. Jung and S. B. Kim, *Vib. Spectrosc.*, 2005, **37**, 33–38.
- 2 M. Kandiah, M. H. Nilsen, S. Usseglio, S. Jakobsen, U. Olsbye, M. Tilset, C. Larabi, E. A. Quadrelli, F. Bonino and K. P. Lillerud, *Chem. Mater.*, 2010, **22**, 6632–6640.
- 3 L. Valenzano, B. Civaleri, S. Chavan, S. Bordiga, M. H. Nilsen, S. Jakobsen, K. P. Lillerud and C. Lamberti, *Chem. Mater.*, 2011, **23**, 1700–1718.
- 4 J. S. Wu, J. S. Wang, H. Y. Li, Y. C. Du, K. L. Huang and B. X. Liu, *J. Mater.*



- Chem. A*, 2013, **1**, 9837–9847.
- 5 H. L. Zhang, X. C. Li, G. H. He, J. J. Zhan and D. Liu, *Ind. Eng. Chem. Res.*, 2013, **52**, 16902–16910.
- 6 S. K. Wu, X. P. Shen, H. Zhou, G. X. Zhu, R. Y. Wang, Z. Y. Ji, K. M. Chen and C. J. Chen, *J. Colloid Interface Sci.*, 2016, **464**, 191–197.